WILEY | Hindawi

Retraction

Retracted: Bioinformatic Deconstruction of Differentially Expressed Sequence Tags in Hepatocellular Carcinoma Based on Artificial Neural Network

Contrast Media & Molecular Imaging

This article has been retracted by Hindawi, as publisher, following an investigation undertaken by the publisher [1]. This investigation has uncovered evidence of systematic manipulation of the publication and peer-review process. We cannot, therefore, vouch for the reliability or integrity of this article.

Please note that this notice is intended solely to alert readers that the peer-review process of this article has been compromised.

Wiley and Hindawi regret that the usual quality checks did not identify these issues before publication and have since put additional measures in place to safeguard research integrity.

We wish to credit our Research Integrity and Research Publishing teams and anonymous and named external researchers and research integrity experts for contributing to this investigation.

The corresponding author, as the representative of all authors, has been given the opportunity to register their agreement or disagreement to this retraction. We have kept a record of any response received.

References

[1] J. Yi, Z. Wen, and Y. Hu, "Bioinformatic Deconstruction of Differentially Expressed Sequence Tags in Hepatocellular Carcinoma Based on Artificial Neural Network," *Contrast Media & Molecular Imaging*, vol. 2022, Article ID 6716324, 12 pages, 2022.

WILEY | Hindawi

Research Article

Bioinformatic Deconstruction of Differentially Expressed Sequence Tags in Hepatocellular Carcinoma Based on Artificial Neural Network

Jing Yi,[1,2] Zhili Wen [1] and Youwen Hu[1]

[1]Department of Gastroenterology, The Second Affiliated Hospital of Nanchang University, Nanchang 330006, Jiangxi, China
[2]Department of Gastroenterology, Jiujiang First People's Hospital, Jiujiang 332000, Jiangxi, China

Correspondence should be addressed to Zhili Wen; haf@bbc.edu.cn

Traditional medical imaging methods for diagnosing hepatocellular carcinoma can only provide information for differential diagnosis in terms of morphology and blood supply of the lesion, and the determination of the nature of the lesion still relies on tissue biopsy. Although ultrasound or CT-guided biopsy has become an effective method for the diagnosis of liver cancer in recent years, the puncture has the possibility of tumor irritation, liver tumor rupture, or needle tract metastasis. In this paper, the use of bioinformatics method is to gradually screen potentially high-risk genes associated with HCC recurrence on a genome-wide scale would help to discover the key target molecules. The ANN method was used to establish a gene prediction model that can predict the recurrence and survival of HCC, so as to construct a tool to identify patients at risk of HCC recurrence. It provided a certain therapeutic basis for future clinical work, thereby improving the prognosis of patients with HCC. Using the "survfit" function of the "survival" package in the R language, the log-rank test (the log-rank test was a common method for comparing two survival curves) was performed on all genes with posthoc recurrence of hepatocellular carcinoma as the outcome event. Then, the BLAST tool (Basic Local Alignment Search Tool) was used to search the similarity of each hepatocellular carcinoma database to find out the genes with similar sequences to each hepatocellular carcinoma, so as to determine the function of each differentially expressed sequence tag. This paper found that the AUC of the ANN model was greater than that of the discriminant analysis model ($P < 0.05$). This paper promoted the development of new therapeutic measures for hepatocellular carcinoma and provided important theoretical guidance for human beings to fight cancer.

1. Introduction

The occurrence of hepatocellular carcinoma is a comprehensive process involving multiple genes and mediated by multiple factors. The natural history of cirrhosis to hepatocellular carcinoma follows a well-established sequence in which dysplastic nodules develop and transform into early and advanced hepatocellular carcinoma. HCC (hepatocellular carcinoma) is not easy to detect in the early stages, and most HCCs are found at an advanced stage. The disease progresses rapidly, the degree of malignant transformation is high, and the prognosis is poor. Over the past decade, many advances have been made in the treatment of HCC. However, the high recurrence rate after these treatments is still a

big problem that is difficult to solve. Therefore, considering the significance of the immune microenvironment in cancer progression, we need to study new immune biomarkers and new immune targets for HCC treatment to provide the basis for early diagnosis, prognostic judgment, and personalized treatment of HCC. The application of bioinformatics to the treatment of HCC in this paper will have an important impact on research in the field of cancer medicine.

CYP2C8 is lowly expressed in HCC tissues and has a correlation with the OS of hepatocellular carcinoma. Zhao et al. discussed the value of sb7-h3 in the differential diagnosis of early stage hepatocellular carcinoma (esHCC) [1]. Qin et al. analyzed the protein components of three liver cancer cell lines by bioinformatics [2]. Yoon et al. described

the experience of pure LRH and compared it with ORH in patients with cirrhotic hepatocellular carcinoma (HCC) [3]. Chen et al. studied the influencing factors of hepatocellular carcinoma [4]. Xiao et al. aims were to examine the role of UCA1 in hepatoma cell proliferation and invasion [5]. However, the treatment method for hepatocellular carcinoma they proposed is not very obvious, and it introduces an artificial neural network to optimize it.

The application of ANN to the diagnosis of hepatocellular carcinoma is still in the research stage. Isik and Inalli used the MATLAB software to model and predict expected data with high sensitivity in thermal systems [6]. Safa et al. used an ANN approach to model wheat production [7]. Ascione et al. optimized the generation of neural networks through uncertainty and sensitivity analysis [8]. Shimabukuro and Semelin explored the impact of network architecture on training quality [9]. Bazan et al. proposed a pattern recognition method for short circuit detection [10]. But their proposed artificial neural network is not accurate enough.

Based on this, the artificial neural network technology is used to deeply mine immune-related genes with prognostic value in HCC patients and then predict and analyze the transcription factors that regulate immune-related genes for HCC independent prognosis. The susceptible biological targets of hepatocellular carcinoma were screened, the biological pathways and their corresponding functions of differentially expressed genes enriched in hepatocellular carcinoma were explored, and the disease modules and their biological functions in the hepatocellular oncoprotein interaction network were explored. The susceptible biological targets of hepatocellular carcinoma were screened by bioinformatics methods, and the biological enrichment pathways related to the progression of hepatocellular carcinoma were found. It provides a scientific and theoretical basis for understanding the occurrence and development of hepatocellular carcinoma from the perspective of molecular cytology. It was found that the fold changes of mRNA of CMTM2 and CMTM6 were −1.721 and −1.655, respectively. The median expression values of core gene mRNA were 1290.13 (TOP2A) and 286.75 (NDC80), respectively.

2. Application of Differentially Expressed Genes Based on Artificial Neural Network in Classification of Hepatocellular Carcinoma

2.1. Hepatocellular Carcinoma. The treatment plan of HCC mainly depends on the location of the tumor, the extent of the lesion, whether there is metastasis, the liver function, and other comprehensive factors. The surgical method is a one-time excision, which can partially remove the liver tumor or liver transplantation, which is currently the only means to cure HCC, and it is the most effective means. When the patient does not meet the surgical requirements because of poor liver function or because of multiple tumors, it cannot be cured by surgery, or there is no healthy and matching liver that can be transplanted.

Therefore, people have to adopt a relatively conservative treatment plan, which can use traditional Chinese medicine, diet therapy. Local treatments such as hepatic artery embolization, cryosurgery, and radiotherapy (including endogenous and exogenous). Of course, early detection and early treatment cannot be achieved. However, there is a lack of treatment methods for advanced patients and the treatment effect is not good. The cancer tissue with a true capsule has a capsule, so the cancer tissue is round, not only grows slowly but also differentiates well. There are many such cancer tissues that have no sign of growth for 1-2 years, and their size is almost unchanged. The original MRI figure of hepatocellular carcinoma used in this paper is in the DICOM (digital imaging and communications in medicine) format of the medical figure, and the figure matrix information needs to be extracted to obtain a two-dimensional figure [11]. The figure is extracted by the trained deep network and finally used for classifier classification. The flowchart of the classification flow figure of hepatocellular carcinoma is shown in Figure 1.

The joint probability distribution of the differential expression of hepatocellular carcinoma in status (v, h) is expressed as follows [12]:

$$p(v, h) = \frac{1}{z} \exp(E),$$
$$z = \sum_{v,h} \exp(E). \tag{1}$$

Among them, z is the normalization factor. If the node states differentially expressed in a certain layer of hepatocellular carcinoma are given, based on the joint probability distribution $P(v, h)$, the conditional distribution of the other layer states can be expressed as follows [13]:

$$p(v_i|h) = \alpha\left(\sum_{j \in h} w_{ij} + h_j\right),$$
$$p(h_j|h) = \alpha\left(\sum_{i \in q} w_{ij} + q_j\right). \tag{2}$$

Among them, $\sigma(\bullet)$ is the sigmoid activation function, and the differentially expressed sequence of hepatocellular carcinoma is defined as follows [14]:

$$\sigma(x) = \frac{1}{1 + \exp(x)}. \tag{3}$$

It seems that for early diagnosis and timely treatment of liver cancer, new therapeutic targets (a drug therapy that stops cancer cells from growing by interfering with specific molecules needed to become cancerous or to grow), and novel diagnostic biomarkers must be found, which is crucial. Once HCC makes progress and breakthroughs, it would be of great significance. In this paper, the transformation formula for the equalization of the histogram of the birth letter analysis would be given as follows [15]:
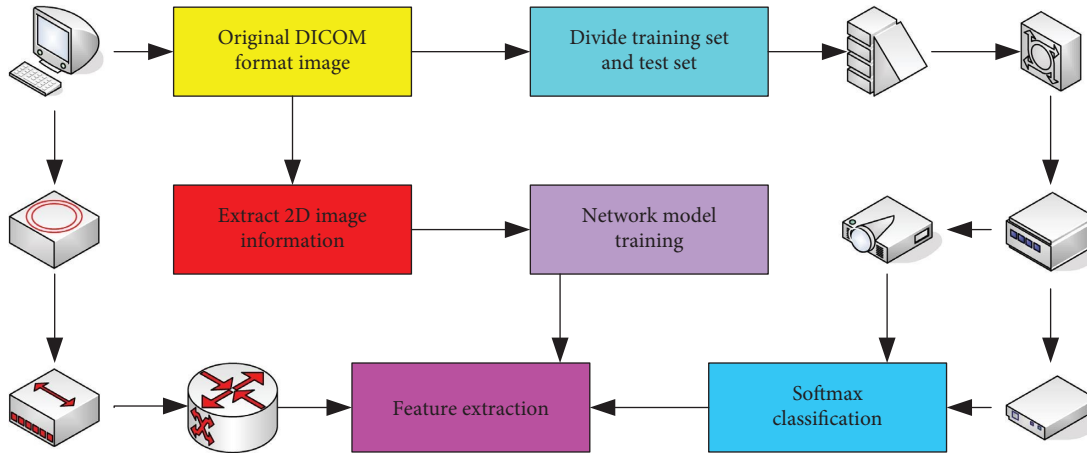
FIGURE 1: Block figure of the hepatocellular carcinoma classification workflow.

$$p_i = \frac{1}{mn} \sum_{x=1}^{m} \sum_{y=1}^{n} \delta * f(x, y). \qquad (4)$$

$$D = \frac{\ln(N(S, \delta))}{\ln(1/\delta)}. \qquad (5)$$

At present, there are three main methods for the clinical diagnosis of liver cancer, namely liver cancer molecular markers, liver biopsy, and various imaging examinations. When the first method is used to test the molecular markers of liver cancer, the sensitivity and specificity of the molecular markers are the keys to the early diagnosis of hepatocellular carcinoma. The higher the sensitivity and the specificity, the greater the significance for the early diagnosis of liver cancer. Therefore, it is necessary to study liver cancer and discover biomarkers that can identify HCC specificity. The second method requires liver puncture, which uses histochemical staining and other cytological and histological examinations. Although it is traumatic, it is more accurate and is often used for the diagnosis of atypical liver cancer or early liver cancer. Because the imaging features are not obvious at this time and the results are in doubt, it is necessary to puncture the tumor. Only after the results are determined can the correct treatment plan be accurately made. However, because of the destruction of the mass, this scheme is likely to cause the movement or metastasis of the destroyed tumor, which theoretically increases the risk of tumor metastasis. The third imaging examination at the time of release is also the first and most commonly used method. These methods do not need to destroy the tumor and have better accuracy than the existing molecular markers. Although various types of imaging examinations have their own advantages and the accuracy of the detection results is also good, it is easy to fail to detect liver cancer in the early stage or when the tumor is not large enough. Among them, the specific contrast agent magnetic resonance imaging technology uses the development of new technology to make up and improve the accuracy of imaging examination for the diagnosis of liver cancer. Assuming that S is any nonempty bounded subset of HCC in R^n, the formula for calculating the box-counting dimension D of S is as follows [16]:

Among them, $N(S, \delta)$ represents the minimum number of boxes required to cover F, and the diameter of the box is δ.

The epidemiological and clinicopathological data of all enrolled patients were collected and included in standardized database management. After recurrence, the choice of treatment is determined by the characteristics of the new lesions and liver function. Treatment options for recurrent lesions confined to the remnant liver include TACE, secondary surgery, and percutaneous radiofrequency ablation (RFA). TACE and RFA can be repeated every 4 weeks. If the tumor invades the main portal vein and inferior vena cava, stereotactic radiotherapy would be given to stabilize the tumor thrombus. When multiple extrahepatic metastases are confirmed, the molecular targeting drug Sorafenib would be used to control disease progression. Active treatment was only given to patients with Child-Pugh (a commonly used clinical grading standard for quantitative assessment of liver reserve function in patients with liver cirrhosis) A or B liver function, and only supportive treatment was given to patients with the Child-Pugh C grade. *Sample inclusion criteria*: patients must not have received interventional embolization, radiofrequency ablation, chemical drugs, or radiation before surgery. The preoperative imaging conformed to the definition of central liver cancer. The postoperative pathological diagnosis was hepatocellular carcinoma and the pathological margin was negative. Single tumor, not associated with large blood vessel invasion and malignant tumors of other organs. Postoperative pathology confirmed that the tumor has no satellite nodules and is not associated with second primary liver cancer. No obvious RNA degradation occurred during the sample collection process (the RNA integrity score was greater than or equal to 5 points by the Agilent 2100 Bioanalyzer system).

Plasma samples from 109 patients with liver cancer were collected from the plasma specimen bank for the validation of candidate markers for prognostic analysis. These plasmas

were frozen at −80°C after extraction. RNA samples were detected by NanoDrop, and the purity required an A260/A280 ratio greater than 1.90. Using the cDNA (complementary DNA) reverse transcribed from the total RNA of the tissue sample as a template. According to the results of the standard curve, it was diluted to an appropriate concentration, and 18S ribosomal RNA was used as the internal reference gene to detect the mRNA expression level of the gene to be tested. Each qPCR reaction was replicated three times in parallel [17].

2.2. Bioinformatic Deconstruction of Differentially Expressed Sequence Tags in Hepatocellular Carcinoma.

The immune microenvironment is a microenvironment formed by infiltrating immune cells in tumor tissue. The key role of the tumor immune microenvironment in immunotherapy and its complexity and richness are gradually recognized by people. In-depth exploration of the tumor immune microenvironment would advance the effect of immunotherapy. The general procedure for differential expression analysis in cells is shown in Figure 2.

Multiple components of the HCC immune microenvironment have been shown to be involved in regulating the biological behavior of HCC. Tumor-infiltrating lymphocytes (TIL) are the main immune components of solid tumors and participate in the host's antitumor response. Most TIL cells are Treg cells. The Treg cells (helper cells) promote immune tolerance to tumor cells. The Treg levels are associated with liver cancer stage and with poorer prognosis of liver cancer patients. In addition, myeloid-derived suppressor cells (MDSC) also play an important role in the regulation and induction of T cells. Knowing more about how DC vaccines act on CD8+ T cells and trigger the host to form a specific antitumor immune response, thereby maximizing their immune induction and regulation potential, may be the key to their immunotherapy. The specific calculation formula of the nonlocal mean is as follows [18]:

$$NL[v](i) = \sum w(i, j) v_{(j)}.$$ (6)

In the formula, $NL[v](i)$ represents the pixel value of the hepatocellular carcinoma pixel point i after the nonlocal mean filtering. Among them, $w(i, j)$ represents the similarity weight of pixels i and j, which satisfies the following relationship [19]:

$$w(i, j) = e^{\dfrac{v(N_i) - v(N_j)}{h}}.$$ (7)

Tumor bioinformatics is an emerging field developed from traditional bioinformatics and clinical informatics in recent years. The purpose of tumor bioinformatics is to discover potential biomarkers and relationships between diseases or individuals and to screen for the key factors in the occurrence and development of cancer. The vast amount of information generated by the new means such as DNA sequencing has led to the importance of data management. Then, through data elaboration and analysis, we seek breakthroughs in biological mechanisms, diagnosis, and

treatment. Proteomic data includes measurements of the total protein expression levels as well as measurements of protein activity, among others. Advances in tumor bioinformatics have greatly contributed to understanding the complex mechanisms of cancer and developing more rational treatment strategies. Bioinformatics can accelerate the identification of drug targets and the screening of drug candidates. High-throughput data such as genomics (an interdisciplinary biological discipline for collective characterization, quantitative research, and comparative study of different genomes of all genes of an organism), genome structure, transcriptomics, and proteomics have all contributed significantly to mechanism-based drug discovery and drug repurposing. In addition, the screening of biomarkers based on tumor bioinformatics has attracted the attention of medical researchers and is an economical and effective method. Advances in bioinformatics technology provide unprecedented opportunities to gain a comprehensive understanding of tumor genomics and ultimately, to enable personalized treatment. The weight update formula is as follows [20]:

$$\Delta w_i(t + 1) = \eta[d - y(t)] x_i.$$ (8)

Among them, η is the learning step size of the perceptron and its value range is (0, 1). Therefore, in order to improve the convergence speed of the perceptron, the method of variable step size is usually adopted. Formulas for calculating medical conditions are as follows [21]:

$$\eta = \sum_{i=1}^{2} w_i(t) x_i - \theta(t) + \alpha.$$ (9)

In the formula, α is a normal quantity, usually taking the value 0.1.

2.2.1. Data Collection and Processing.
Log in to the immunology database and analysis portal, click on Resources and download all immune-related gene names through Gene Lists. Next, copy the downloaded immune-related gene names to matrix 2 and use the if (COUNTIF) function in Excel to extract the immune-related genes. This results in a matrix (Matrix 3) in which the row names are immune-related gene names and the column names are sample names.

2.2.2. Differential Expression Analysis of Immune-Related Genes.
The criteria for screening differential immune-related genes were |log2foldchange| > l and adjusted P value <0.05. The "org.Hs.cg.db" package was applied in R to transform the differentially expressed immune-related gene names into the corresponding gene ID. Install the R packages "clusterProfiler," "enrichplot," "ggplot2" and use the obtained differentially expressed immune-related gene ID files as input files to perform the GO and KEGG enrichment analysis (according to the concentration of its genes, it can be inferred which phenotype is closer to the known function) in R. The calculation formula of the convolutional layer is as follows [22]:
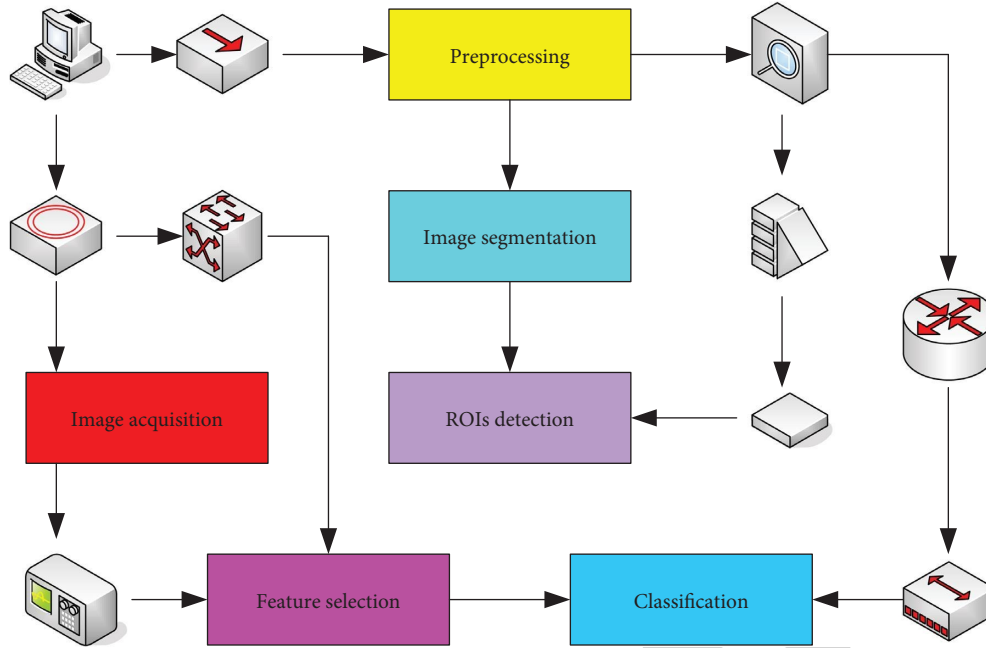
FIGURE 2: General procedure for differential expression analysis in cells.

$$h_j^l = F\left(b^l + \sum_{k=1}^{i} w_{kij}^l\right). \tag{10}$$

2.2.3. Survival Analysis of Differentially Expressed Immune-Related Genes in Hepatocellular Carcinoma. In this study, survival analysis was performed for HCC patients with a follow-up time of no more than 2000 days. In the R software, Kaplan–Meier survival analysis (KM method) and the univariate Cox analysis method (Cox method) were used to find survival-related differentially expressed immune-related genes. The KM method treats genes as discrete variables and is one of the most commonly used methods for survival analysis. The KM method is to divide the samples into two groups according to the median value of gene expression, and whether the gene was associated with survival was judged according to the obtained P value. Its core function is the survdiff function. The univariate Cox analysis method regards genes as continuous variables and is mainly used for the prognosis analysis of tumors and many chronic diseases. The Cox method analyzed the correlation between gene expression and survival time and survival status decided whether the gene expression was related to survival according to the obtained P value. The core function for calculating the Cox model is the coxph function. The results of KM survival analysis and Cox methods are not necessarily related. After searching by the two methods, the Venn figure was drawn by the online tool VENNY 2.0, and the differentially expressed immune-related genes were obtained. The formula for the Softmax function is as follows:

$$f(x_i) = \sum_{i,j=1}^{k} e^{x_{ij}}. \tag{11}$$

2.2.4. Screening of Independent Prognostic Genes. Genes that can be used as independent prognostic factors are very meaningful for judging the treatment status and prognosis of patients. To determine whether genes associated with survival could serve as independent prognostic factors, each gene obtained in the previous step was combined with clinical data (age, gender, grade, pathological stage, and T stage) to perform the multivariate Cox analysis. The P value less than 0.01 was used as the screening condition to screen out independent prognostic immune-related genes. A forest plot was drawn showing the hazard ratio (HR), 95% confidence interval, and P value of each independent prognostic immune-related gene and clinical data. To train the autoencoder, a loss function is constructed by minimizing the mean square reconstruction error:

$$J(w, b, \widetilde{b}) = \frac{\sum_{i=1}^{N} \|x_i\|^2}{n}. \tag{12}$$

2.2.5. Predictive Analysis of Transcription Factors Regulating Immune-Related Genes Independent of Prognosis in HCC. We extracted 318 transcription factors from the cis-trans cancer database for prognostic immune-related genes research. First, use the if(COUNTIF) function in Excel to extract transcription factors from matrix 2, so as to obtain a matrix (matrix 4) whose row names are transcription factor names and column names are sample names. Then, the KM survival analysis and univariate Cox analysis were used to find survival-related differential transcription factors in R software. After using the two methods to find, use the online tool VENNY 2.0 to draw a Venn figure and get the transcription factors with prognostic value that the two methods coexist. Normal samples were deleted and HCC tissue samples were retained. The correlations between prognosis-

related TFs and prognosis-immunity-related genes were then obtained using the cor.test function in R. The Cytoscape software is used to build and visualize the regulatory network so as to obtain the network figure of transcription factors regulating immune-related genes of HCC independent prognosis.

2.3. Algorithm for Differentially Expressed Sequence Tagging of Hepatocellular Carcinoma Based on Artificial Neural Network. With the in-depth study of the artificial neural network theory and the rapid development of electronic computer application technology, its theory has gradually matured, especially its application in the field of medical research, which is also gradually expanding. Artificial neural network is superior to conventional statistical methods, it does not necessarily require the original data to be normally distributed. Furthermore, it has a certain fault tolerance for the defects of individual measurement values in the determination process. These advantages bring great convenience to the popularization of neural networks. According to the conventional statistical methods, the more the combined markers, the higher the positive rate and the higher the false positive rate. The application of artificial neural network technology can not only improve the positive rate of liver cancer diagnosis but also improve its specificity and can take into account both at the same time.

Assuming that the input of the i-th neuron in the $k - 1$ layer is $y_i^{(k-1)}$ and the output is $y_i^{(k)}$, the relationship between the input and output of differential expression in hepatocellular carcinoma is as follows:

$$y_j^{(k)} = f\left(\sum_{i=1}^{N_k} w_{ij}^k * y_i^{k-1} + \theta^{(k)}\right). \tag{13}$$

Among them, $w_{ij}^{(k-1)}$ is the connection weight between the ANN neurons. The expression of the fusion of differentially expressed signatures in hepatocellular carcinoma can be defined as follows:

$$Y = F[X_1, X_2]. \tag{14}$$

In the formula, X_1 and X_2, respectively, represent the features learned by the two network models. In practical problems, the probability distribution $P(v)$ of the observed data v is related to the performance of the network model. The greater its probability, the better the restoration effect of the trained network model on the observed data. It corresponds to the marginal distribution of the probability $P(v, h)$, it can be obtained as follows:

$$p(v) = \sum_{h=1} p(v, h). \tag{15}$$

Assuming that the number of hidden layers of the DBN model is N, based on the joint probability distribution, the relationship between the input data v and the hidden vector can be expressed as follows:

$$p(v, h^N) = \prod_{k=1}^{N-1} p(h^k|h) p(h^N). \tag{16}$$

The formula for the gradient of the convolutional layer is as follows:

$$\delta_j^i = \tau_j^{i+1}\left(f(u_j^i) \bullet p(\delta_j^{i+1})\right),$$
$$u_j^i = w_j^i x_j^{i-1}. \tag{17}$$

First, from forward propagation, the input variable information of differential expression of hepatocellular carcinoma is transmitted from the input layer to the output layer through the processing of the hidden layer, and the state of each layer of neurons only affects the state of the lower layer of neurons. If the expected error result is not obtained in the input layer of differentially expressed sequence tags in hepatocellular carcinoma, it would return according to the original propagation path, that is, back propagation. After modifying the weights of neurons in each layer, the desired output is achieved. Use 5 tumor markers as input variables and normalize the raw data before input. 1 output variable, defined as 0.9 for liver cancer, 0.5 for benign, and 0.1 for normal. The preset number of network training cycles is 3000, the set training error is 0.001; the learning rate is 0.7, and the preset value of the momentum factor is 0.95.

3. Bioinformatic Deconstruction Results of Differentially Expressed Sequence Tags in Hepatocellular Carcinoma

The analysis showed that DEGs in the HCC group and the control group were mainly enriched in mitotic spindle (NES = 1.611, NOMp-val = 0.002, and FDR = 0.214), G2M checkpoint (NES = 1.553, NOMp-val = 0.004, and FDR = 0.125), and it also has gene sets such as E2F targets (NES = 1.540, NOMp-val = 0.004, and FDR = 0.070), spermatogenesis (NES = 1.550, NOMp-val = 0.020, and FDR = 0.097), and DNA repair (NES = 1.578, NOMp-val = 0.032, and FDR = 0.151). The GSEA database analysis is shown in Figure 3.

Subsequently, the relationship between the different expression values of each core gene and the survival of patients were analyzed. The analysis results are shown in Figure 4. The P values of the nine core genes and patient survival analysis were 0.0042 (TOP2A), 0.0012 (NDC80), 0.0012 (CDKI), 0.00024 (CCNBL), 0.00044 (KIF11), and 0.00015 (BUB1). Among them, Bub1, CCNBI, and KIF1I have the most significant statistical difference. There were differences in the distribution of visible mRNA expression in different age, race, histological type, pathological stage, tumor recurrence, and survival status ($P < 0.05$). There is little difference in distribution among different genders and grades.

CMTM2 and CMTM6 mRNA's fold changes were −1.721 and −1.655. The expression levels of CMTMs mRNA in hepatocellular carcinoma are shown in Table 1.
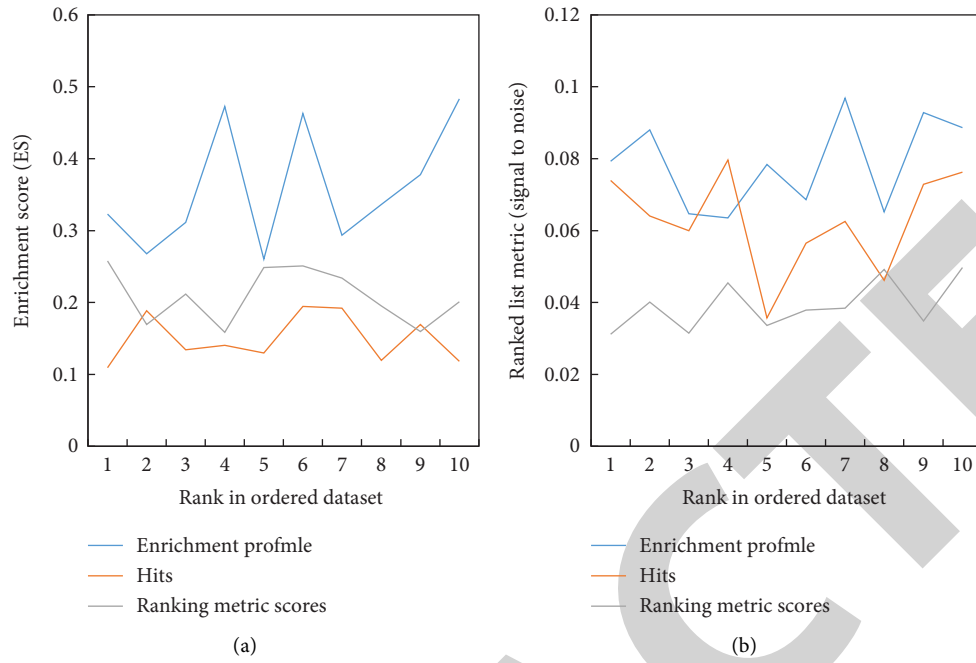
FIGURE 3: GSEA database analysis. (a) Enrichment fraction. (b) Ranked list metrics.
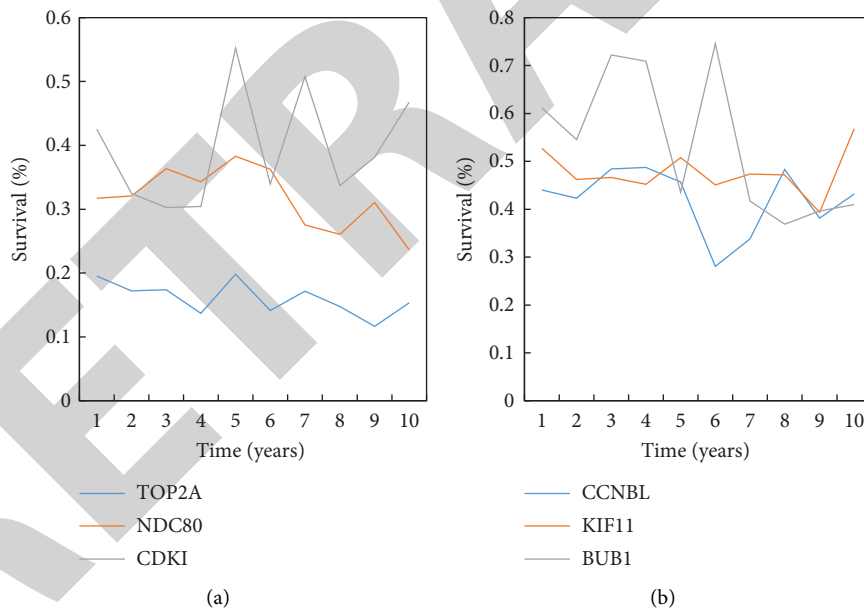

FIGURE 4: The relationship between different expression values of each core gene and patient survival. (a) TOP2A, NDC80, and CDK1. (b) CCNB1, KIFII, and BUBI.

TABLE 1: Expression levels of CMTMs mRNA in hepatocellular carcinoma.

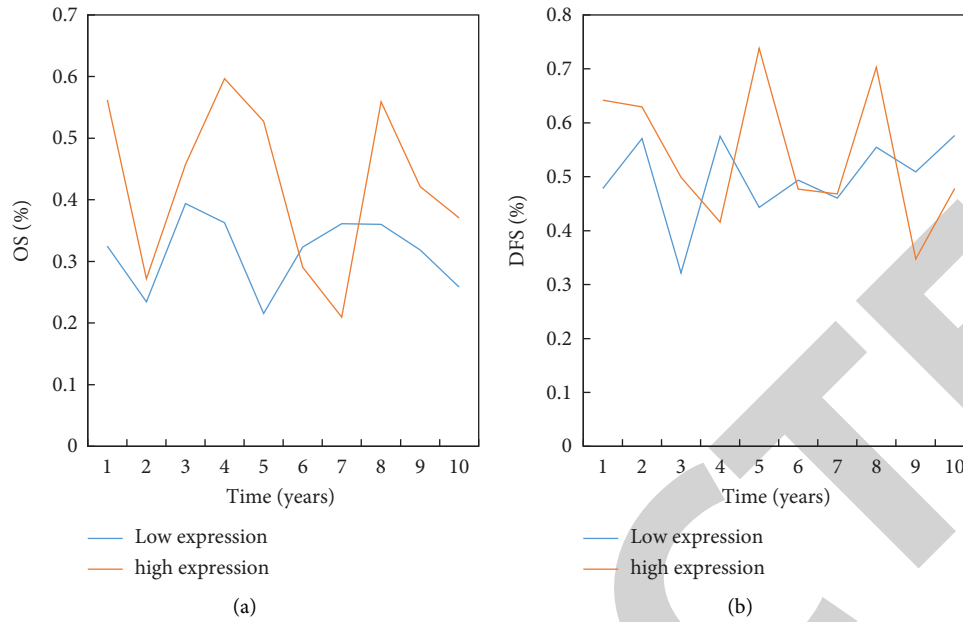| Organization type	Change factor	t
Hepatocellular carcinoma	1.2	7.481
Cirrhosis	1.6	16.661
Hepatocellular carcinoma	1.7	5.028
Atypical hyperplasia of hepatocytes	2.1	7.748

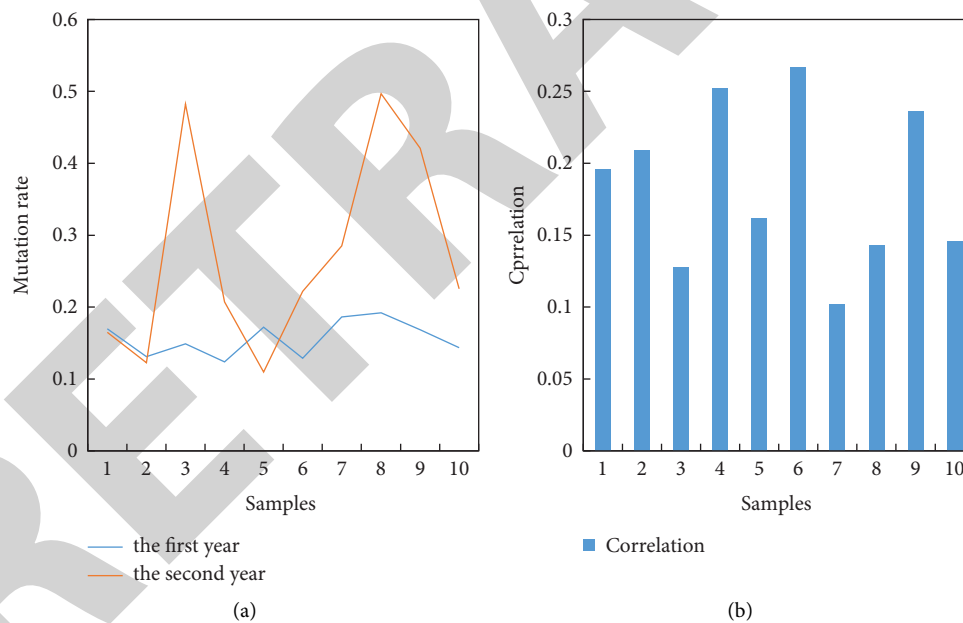Figure 5: Effect of CMTMs on survival of HCC patients. (a) OS. (b) DFS.

Figure 6: CMTMs gene mutation and its correlation with the survival of patients with hepatocellular carcinoma. (a) Gene mutation of CMTMs. (b) Correlation of survival in patients with hepatocellular carcinoma.

After clarifying the differential expression of CMTMs mRNA and protein levels, the effect of CMTMs (CKLF-like MARVEL transmembrane domain-containing) on the survival of HCC patients is shown in Figure 5.

With the help of the cBioPortal database, we determined the gene mutation frequencies of nine CMTMs in HCC patients. A total of 102 (29.57%) of all HCC patients carried CMTMs gene mutations, and the main types included amplification, missense mutations, and up- and down-

regulation of transcription levels. In addition, the cBioPortal database was used to study the correlation between CMTMs gene mutation and prognosis of HCC patients. CMTMs gene mutations in HCC patients are closely related to OS and DFS. The OSand DFS of HCC patients with CMTMs mutation were significantly worse than those without CMTMs mutation. The CMTMs gene mutation and its correlation with the survival of patients with hepatocellular carcinoma are shown in Figure 6.
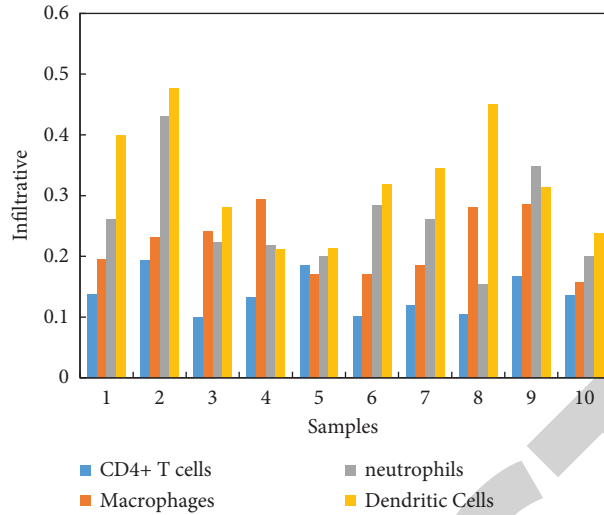
Figure 7: Correlation between CMTMs and immune cell infiltration.

Table 2: HR values of key genes.

Gene name	HR value	P(HR) value
AURKA	1.11	0.16
CDKN3	1.21	0.1
PRC1	1.46	0.12
NCAPG	0.21	0.001

Table 3: ANN model discrimination results.

Evaluation indicators	ANN model	Discriminant analysis model
Sensitivity	95.0%	45.0%
Specificity	97.3%	97.2%
Accuracy	94.3%	69.3%
Total positive predictive value	97.0%	95.7%
Total negative predictive value	96.7%	65.6%
Area under the ROC curve	0.975	0.742
(95% confidence interval)	0.957~1.005	0.664~0.910

Considering that inflammatory response and immune cell infiltration can affect the prognosis of HCC patients, the correlation between CMTMs and immune cell infiltration was evaluated by the TIMER database as shown in Figure 7. These findings provide strong evidence that CMTMs play a special role in the immune infiltration of HCC.

The first three genes with less distribution of cancer types were selected, and PROZ, HGFAC, and SLC22A1 were finally identified as highly specific key genes for further research and analysis. The HR values of key genes are shown in Table 2.

The specificity and total positive predictive value of ANN and discriminant analysis model are equal or close to each other, while the other three items are quite different. By comparing the AUC of their respective ROC curves, it was found that the AUC of the ANN model was greater than that of the discriminant analysis model ($P < 0.05$). The discriminative results of the ANN model are shown in Table 3.

Five indicators were tested by Kolmogorov–Smirnov and Shapiro–Wilk for normality, and only the concentration of sialic acid (SA) obeyed the normal distribution, and the concentration values of the other four indicators were all skewed distribution. The concentration difference of SA among the three groups were greater than 0.05 by variance analysis ($P = 0.177$). The P value ($P = 0.001$) of the remaining 4 indicators were all less than 0.05 by non-parametric test and it could be considered that the differences among the 3 groups of the 4 indicators were statistically significant. The test results of AFP, CEA, and SA are shown in Table 4.

Kaplan–Meier survival analysis of HCC patients was performed for three genes in the Kaplan–Meier plotter database. All HCC patients using this database were analyzed and it was found that the expression levels of HGFAC (HR = 0.65, $P = 0.0149$), PROZ (HR = 0.59, $P = 0.0027$), and SLC22A1 (HR = 0.52, $P = 0.0002$) in patients with

TABLE 4: AFP, CEA, and SA test results.

Group	AFP (μg/L)	CEA (μg/L)	SA (μg/L)
Normal group	1.8	10	805
Liver benign group	0.9	6	822
Liver cancer group	22	30	831

hepatocellular carcinoma were correlated with the OS in patients with HCC. The lower the expression level, the worse the prognosis. Expressions of PROZ (HR = 0.24, $P = 1.5 \times 10 - 0.5$) and SLC22A1 (HR = 0.24, $P = 7.9 \times 10 - 6$) in Asian HCC patients were correlated with the OS. The lower the expression level, the worse the prognosis. Although the expression of HGFAC (HR = 0.69, $P = 0.2157$) was correlated with the OS of patients, it was not statistically significant. The expression of SLC22A1 (HR = 0.45, $P = 0.0212$) in HCC patients with hepatitis was correlated with the OS, and the lower the expression, the worse the prognosis. However, the correlation between HGFAC (HR = 1, $P = 0.996$) and PROZ (HR = 0.74, $P = 0.3635$) and OS was not statistically significant. The expression of SLC22A1 (HR = 0.52, $P = 0.0422$) in HCC patients with a history of alcohol intake was correlated with the OS, the lower the expression, the worse the prognosis. However, the correlation between HGFAC (HR = 0.76, $P = 0.3925$) and PROZ (HR = 0.54, $P = 0.0602$) and the OS was not statistically significant. Figure 8 shows the relationship between the gene expression and the overall survival (OS) of patients with hepatocellular carcinoma.

The LinkedOmics database downloads the gene expression data of TNM staging and pathological staging of the three key genes of all hepatocellular carcinoma patients. The stability and consistency of the correlation between the expression level of PROZ gene and TNM staging showed the best performance. It can be roughly seen that the lower the expression level of PROZ gene, the later the TNM staging. SLC22A1 and HGFAC showed poor stability in the correlation with TNM staging and the trend was not clear. In the results of pathological staging, we can see that the expression levels of PROZ and SLC22A1 have better stability and consistency in correlation with pathological staging. However, the stability of the correlation between HGFAC and pathological staging was poor and the trend was not clear. The gene expression data of TNM staging and pathological staging of the three key genes in patients with hepatocellular carcinoma are shown in Figure 9.

Among the classification results obtained in this paper, the accuracy, sensitivity, and specificity of the axial position are the highest. Compared with the coronal position and the anamorphic position, the difference is 6 or 7 percentage points. This is also in line with the actual sampling data. The three-dimensional view of hepatocellular carcinoma is usually reconstructed from serial MRI images scanned in the axial direction. Therefore, the axial images are generally relatively clear, while the coronal and anamorphic images are usually obtained by resampling the reconstructed 3D views. Therefore, it is inferior to the axial position in terms of clarity and naturally has a large gap with the axial position in the classification performance. In the traditional method, the
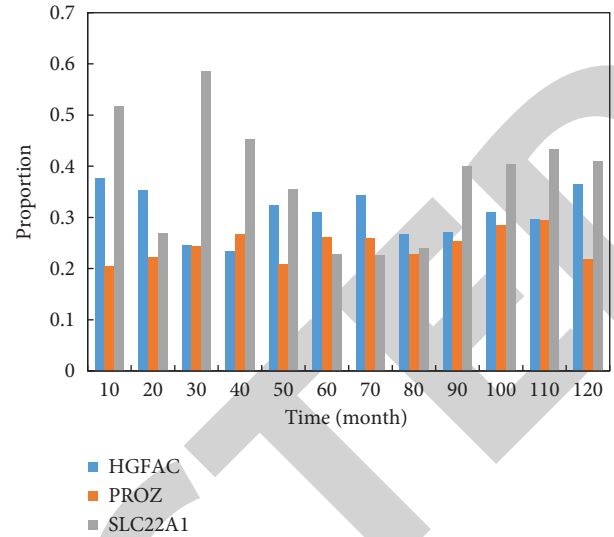

FIGURE 8: Relationship between the gene expression and overall survival (OS) in patients with hepatocellular carcinoma.
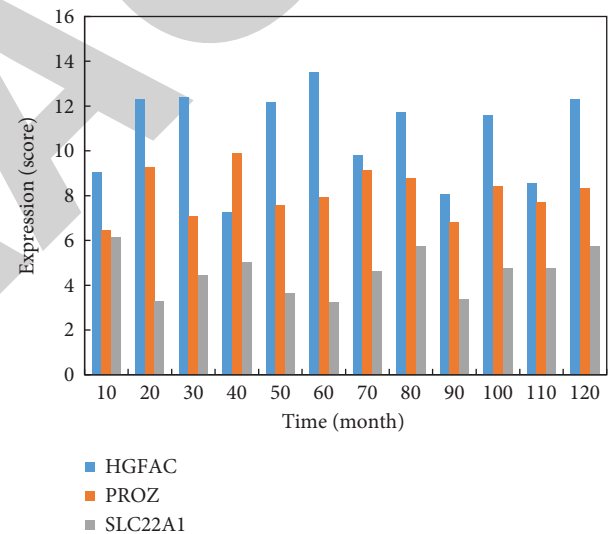

FIGURE 9: Gene expression data of TNM staging and pathological staging of the three key genes in patients with hepatocellular carcinoma.

hepatocellular carcinoma figure is preprocessed, the texture features are extracted, and then the corresponding classifier is selected for classification. It is also necessary to manually design which feature to extract, which is not only time-consuming and labor-intensive but also does not necessarily obtain satisfactory results. The convolutional artificial neural network used in this paper for classification only needs to input the training set and test set into the network. Given the error optimization function, the network can continuously adjust the weight parameters during training to make the network model optimal. In the process, there is no need to manually design feature methods, nor do we need to manually extract features and select classifiers, and the final result exceeds the classification effect of texture features. The local feature classification results are shown in Table 5.

TABLE 5: Local feature classification results.

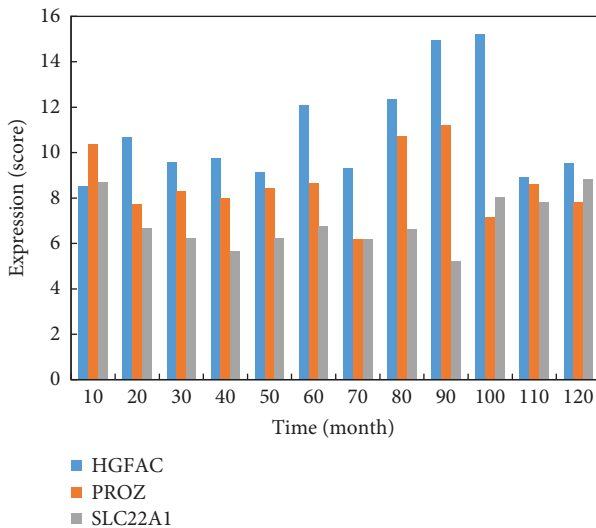| Feature method	Accuracy (%)	Sensitivity (%)	Specificity (%)
Axial position	78.95	71.45	77.86
Coronal	81.08	71.68	86.40
Lost bit	74.67	70.35	71.71

FIGURE 10: Gene expression data of TNM staging and pathological staging in Asian HCC patients based on the three key genes.

Figure 10 shows the gene expression data of the three key genes in TNM staging and pathological staging of Asian HCC patients. It was found that the expression levels of PROZ and SLC22A1 were correlated with TNM staging, and the stability and consistency were better. The lower the expression levels of PROZ and SLC22A1, the later the TNM staging. The stability of the correlation of the HGFAC gene in TNM staging was poor and the trend was not clear. The lower the expression levels of PROZ and SLC22A1, the later the pathological stage. The stability of the correlation between HGFAC and pathological stage was poor and the trend was less clear.

4. Conclusion

The prevalence of HCC was very high, but most patients with liver cancer were found in the middle and late stages, and patients with advanced HCC have few treatment options and poor treatment effect. Therefore, early detection and diagnosis, exploring the key genes of HCC pathogenesis and pathways, and finding new targeted therapies are of great significance for improving the prognosis of HCC patients, and will definitely become the main goal of future research. At present, the application of the artificial neural network in the diagnosis of hepatocellular carcinoma is still in the research stage. In this paper, the bioinformatics changes of normal liver tissue, liver cirrhosis, and hepatocellular carcinoma were observed, and the large amount of data generated by differentially expressed sequence tags of hepatocellular carcinoma was processed by the artificial neural network. The effect of the artificial neural network on improving the diagnostic accuracy of bioinformatics analysis was studied. Although great efforts have been made to find new biomarkers and many new serum markers have been proposed to assist in the diagnosis and treatment of HCC, there is still no single ideal marker in HCC. There were obvious pitfalls and deficiencies in using a single biomarker to diagnose early-stage liver cancer. Combining multiple tumor markers as detection standards in future work can significantly improve the sensitivity and specificity of early diagnosis of liver cancer and with the deepening of molecular biology research, new liver cancer markers will continue to be discovered.

Data Availability

The datasets generated during and/or analyzed during the current study are not publicly available due to sensitivity and data use agreement.

Conflicts of Interest

The authors declare that there are no conflicts of interest.

References

[1] L. Zhao, C. Xie, D. Liu, T. Li, Y. Zhang, and C. Wan, "Early detection of hepatocellular carcinoma in patients with hepatocirrhosis by soluble B7-H3," *Journal of Gastrointestinal Surgery*, vol. 21, no. 5, pp. 807–812, 2017.

[2] G. Qin, M. Dang, H. Gao, H. Wang, F. Luo, and R. Chen, "Deciphering the protein-protein interaction network regulating hepatocellular carcinoma metastasis," *Biochimica et Biophysica Acta, Proteins and Proteomics*, vol. 1865, no. 9, pp. 1114–1122, 2017.

[3] Y. I. Yoon, K. H. Kim, S. H. Kang et al., "Pure laparoscopic versus open right hepatectomy for hepatocellular carcinoma in patients with cirrhosis," *Annals of Surgery*, vol. 265, no. 5, pp. 856–863, 2017.

[4] W. Chen, L. Ye, D. Wen, and F. Chen, "MiR-490-5p inhibits hepatocellular carcinoma cell proliferation, migration and invasion by directly regulating ROBO1," *Pathology and Oncology Research*, vol. 25, no. 1, pp. 1–9, 2017.

[5] J. N. Xiao, T. H. Yan, R. M. Yu et al., "Long non-coding RNA UCA1 regulates the expression of Snail2 by miR-203 to promote hepatocellular carcinoma progression," *Journal of Cancer Research and Clinical Oncology*, vol. 143, no. 6, pp. 981–990, 2017.

[6] E. Isik and M. Inalli, "Artificial neural networks and adaptive neuro-fuzzy inference systems approaches to forecast the meteorological data for HVAC: the case of cities for Turkey," *Energy*, vol. 154, no. JUL.1, pp. 7–16, 2018.

[7] M. Safa, S. Samarasinghe, and M. Nejat, "Prediction of wheat production using artificial neural networks and investigating indirect factors affecting it: case study in canterbury province, New Zealand," *Journal of Agricultural Science and Technology A*, vol. 17, no. 4, pp. 791–803, 2018.

[8] F. Ascione, N. Bianco, C. De Stasio, G. M. Mauro, and G. P. Vanoli, "Artificial neural networks to predict energy performance and retrofit scenarios for any member of a building category: a novel approach," *Energy*, vol. 118, no. JAN.1, pp. 999–1017, 2017.

[9] H. Shimabukuro and B. Semelin, "Analysing the 21cm signal from the Epoch of Reionization with artificial neural networks," *Monthly Notices of the Royal Astronomical Society*, vol. 468, no. 4, pp. 3869–3877, 2017.

[10] G. H. Bazan, P. R. Scalassara, W. Endo, A. Goedtel, W. F. Godoy, and R. H. C. Palacios, "Stator fault analysis of three-phase induction motors using information measures and artificial neural networks," *Electric Power Systems Research*, vol. 143, no. Feb, pp. 347–356, 2017.

[11] A. C. Gardini, F. G. Foschi, F. Conti et al., "Immune inflammation indicators and ALBI score to predict occurrence and recurrence of hepatocellular carcinoma in HCV-related cirrhosis treated with direct-acting antivirals," *Digestive and Liver Disease*, vol. 50, no. 1, pp. 50-51, 2018.

[12] K. Ikeda, M. Kudo, S. Kawazoe et al., "Phase 2 study of lenvatinib in patients with advanced hepatocellular carcinoma," *Journal of Gastroenterology*, vol. 52, no. 4, pp. 512–519, 2017.

[13] C. Bosetti, C. Bianchi, E. Negri, M. Colombo, and C. La Vecchia, "Estimates of the incidence and prevalence of hepatocellular carcinoma in Italy in 2002 and projections for the years 2007 and 2012," *Tumori Journal*, vol. 95, no. 1, pp. 23–27, 2018.

[14] U. G. Rossi and M. Cariati, "Transarterial embolization for hepatocellular carcinoma: reasoning on mechanisms of action, tips and tricks of the procedure," *European Journal of Gastroenterology and Hepatology*, vol. 29, no. 4, pp. 488-489, 2017.

[15] T. Jiang, M. Li, Q. Li et al., "MicroRNA-98-5p inhibits cell proliferation and induces cell apoptosis in hepatocellular carcinoma via targeting IGF2BP1," *Oncology Research Featuring Preclinical and Clinical Cancer Therapeutics*, vol. 25, no. 7, pp. 1117–1127, 2017.

[16] M. Kudo, E. Hatano, S. Ohkawa et al., "Ramucirumab as second-line treatment in patients with advanced hepatocellular carcinoma: Japanese subgroup analysis of the REACH trial," *Journal of Gastroenterology*, vol. 52, no. 4, pp. 494–503, 2017.

[17] E. Rinninella, L. Cerrito, I. Spinelli et al., "Chemotherapy for hepatocellular carcinoma: current evidence and future perspectives," *Journal of Clinical and Translational Hepatology*, vol. 5, no. XX, pp. 1–14, 2017.

[18] X. Fu, H. Wen, L. Jing et al., "MicroRNA-155-5p promotes hepatocellular carcinoma progression by suppressing PTEN through the PI3K/Akt pathway," *Cancer Science*, vol. 108, no. 4, pp. 620–631, 2017.

[19] P. J. Zamor, A. S. Delemos, and M. W. Russo, "Viral hepatitis and hepatocellular carcinoma: etiology and management," *Journal of Gastrointestinal Oncology*, vol. 8, no. 2, pp. 229–242, 2017.

[20] Y. S. Ma, T. M. Wu, Z. W. Lv et al., "High expression of miR-105-1 positively correlates with clinical prognosis of hepatocellular carcinoma by targeting oncogene NCOA1," *Oncotarget*, vol. 8, no. 7, pp. 11896–11905, 2017.

[21] J. Howell, D. J. Pinato, R. Ramaswami et al., "On-target sorafenib toxicity predicts improved survival in hepatocellular carcinoma: a multi-centre, prospective study," *Alimentary Pharmacology & Therapeutics*, vol. 45, no. 8, pp. 1146–1155, 2017.

[22] A. Khorasani and M. R. S. Yazdi, "Development of a dynamic surface roughness monitoring system based on artificial neural networks (ANN) in milling operation," *International Journal of Advanced Manufacturing Technology*, vol. 93, no. 1-4, pp. 141–151, 2017.